draft date: January 14, 2014

Protostars in the Elephant Trunk Nebula

William T. Reach[1] Jeonghee Rho[1] Erick Young[3] James Muzerolle[3] Sergio Fajardo-Acosta [1] Lee Hartmann[4] Aurora Sicilia-Aguilar[4] Lori Allen[4] Sean Carey[1] Jean-Charles Cuillandre[6] Thomas H. Jarrett[2] Patrick Lowrance[1] Anthony Marston[5] Alberto Noriega-Crespo[1] Robert L. Hurt[1]

reach@ipac.caltech.edu

ABSTRACT

The optically-dark globule IC 1396A is revealed using *Spitzer* images at 3.6, 4.5, 5.8, 8, and 24 μm to be infrared-bright and to contain a set of previously unknown protostars. The mid-infrared colors of the 24 μm detected sources indicate several very young (Class I or 0) protostars and a dozen Class II stars. Three of the new sources (IC 1396A:γ, δ, and ϵ) emit over 90% of their bolometric luminosities at wavelengths greater than 3 μm, and they are located within ~ 0.02 pc of the ionization front at the edge of the globule. Many of the sources have spectra that are still rising at 24 μm. The two previously-known young stars LkHα 349 a and c are both detected, with component c harboring a massive disk and component a being bare. Of order 5% of the mass of material in the globule is presently in the form of protostars in the 10^5–10^6 yr age range. This high star formation rate was likely triggered by radiation from a nearby O star.

[1] *Spitzer* Science Center, MS 220-6, California Institute of Technology, Pasadena, CA 91125

[2] Infrared Processing and Analysis Center, MS 100-22, California Institute of Technology, Pasadena, CA 91125

[3] Steward Observatory, University of Arizona, Tucson AZ

[4] Smithsonian Astrophysical Observatory, 60 Garden St., Cambridge, MA 02138

[5] European Space Research and Technology Center, Noordwijk, Netherlands

[6] Canada-France-Hawaii Telescope, HI

1. Introduction

To demonstrate the capabilities of the new *Spitzer* Space Telescope (Werner et al. 2004), the facility scientists observed some targets that are dark at optical wavelengths but expected to be bright in the infrared. The Elephant Trunk Nebula is a textbook example of a dark globule immersed in an H II region: see Figs. 7.3 and 7.4 of Osterbrock (1974). The H II region is IC 1396, a large (100′ diameter) ionized region within an infrared-bright shell. An excellent summary of knowledge of this region was written by Weikard et al. (1996). The distance to IC 1396 is estimated at 750 pc. Comparing the radio and Hα brightness of the H II region, it appears there is only about 1.2 mag of spatially uniform foreground extinction (Morbidelli et al. 1997). The region is ionized by the O6 star HD 206267, and it is joined by 20 B stars in the cluster Trumpler 37. Radiation and winds from these stars sculpt the dense molecular gas into a variety of shapes with a predominant cometary morphology where the dense head points roughly back toward the O6 star.

The most prominent globules are located in the western and northern portions of the H II region. The rims of these globules are bright in Hα, as seen in red optical images, demarking the gradual progress of the ionization front from the O6 star into the globule. The surfaces of the globules are also illuminated by scattered starlight, most easily visible in blue optical images. A three-color optical image of the Elephant Trunk Nebula from the Canada-France-Hawaii Telescope (CFHT) is shown in the inset of Plate 1. These globules were notable for being dark, but the combination of dense material (required to harbor enough dust to extinguish all background starlight) and a source of radiation and pressure (required to make the bright rims) makes the globules very likely locations of recent star formation. The swept-back appearance of the globules is related to radiation and wind pressure from the central O star. The globules are very bright in CO emission (Patel et al. 1995) and have atomic 'tails' that extend up to 6 pc opposite the central star (Moriarty-Schieven, Xie, & Patel 1996). Two globules, IC 1396N and IC 1396W, exhibit recent star formation with outflows and new Herbig-Haro objects (Reipurth et al. 2003; Froebrich & Scholz 2003). The Elephant Trunk Nebula, IC 1396A, contains two T Tauri stars (Cohen & Kuhi 1979; Herbig & Bell 1988). The new observations presented here reveal prolific, recent star formation by uncovering a host of new, infrared-bright protostars.

2. Observations

IC 1396 was observed at 3.6–8 μm on 2003 Nov 5 using IRAC (Fazio et al. 2004) [ads/sa.spitzer#0006051840]. The IRAC observations have 2 sec frames and the map grid has 1/2-array spacings in each direction, yielding a total observing time per sky position

of 8 sec; the IRAC map took 21 min of wall-clock time. IC 1396 was observed at 24 μm on 2003 Nov 24 using MIPS (Rieke et al. 2004) [ads/sa.spitzer#0006052096]. The MIPS observations have 3 sec frames and used the small-field photometry mode with a 3×3 raster, yielding a total observing time per sky position of 42 sec; the MIPS map took 17 minutes. The photometric accuracy of the IRAC and MIPS data is better than 10%. For the point source photometry, *Spitzer* and 2MASS magnitudes are accurate to better than 0.1 and 0.05 magnitudes, respectively.

3. Dust and gas in the globule

The mid-infrared images reveal the body of the globule, which is dark in optical photographs, as brilliant, structured emission (Plate 1). The inner edge of the rim of the globule, dark in the optical images, is bright in the infrared. The bright eastern rim faces the O6 star. Within the head of the bright globule, there is a circular cavity containing LkHα 349; that this is a cavity is known from microwave CO spectroscopy (Nakano et al. 1989).

The brightness, subtracting a background in a faint part of the image, ranges from 4.5–31 MJy sr^{-1} at 24 μm, from individual filaments in the south to the globule rim in the east. The ratio of the IRAC 8 μm to MIPS 24 μm surface brightness (I_ν) ranges from 1.4 to 2.6, with the lower ratio being common and the higher ratio applying in the region just west of the densest part of the globule (green region in Fig. 1). For comparison, the diffuse interstellar spectrum, convolved with *Spitzer* wavebands, has a ratio $\sim$ 1.2 (Ingalls et al. 2004), similar to the bulk of the globule emission (brownish red in Fig. 1). The other color ratios are $I_\nu(3.6, 4.5, 5.8)/I_\nu(8) = 0.1$, 0.05, 0.3.

The mid-infrared emission is a combination of small grains, polycyclinc aromatic hydrocarbon (PAH), and H_2 lines. Archival ISOCAM imaging spectroscopy from 5–17 μm shows that the IRAC 5.8 and 8 μm bands are dominated by PAH features at 6.2 and 7.7 μm typical for interstellar lines of sight (Boulanger et al. 2004). The ISOCAM spectra also detect pure rotational H_2 lines, which contribute $\sim$ 2% and $\sim$ 8% in the 8 μm and 5.8 μm bands, respectively. At shorter wavelengths, using a simple model based on IC 443 molecular shocks (Rho et al. 2001), we estimate H_2 lines contribute $\sim$ 50% and $\sim$ 30% of the 4.5 μm and 3.6 μm bands, respectively. Though the H_2 excitation is uncertain, it appears the 4.5 μm band could be a good tracer of H_2 emission. That the 4.5 μm is similar to the others suggests the H_2 and dust emission are reasonably well correlated. However, some of the mid-infrared color variation in Figure 1 is likely due to the relative brightness of H_2 compared to dust emission.

4. Stars in and near the globule

The optically-bright star inside the cavity in IC 1396A is LkHα 349a. This star may have cleared the central cavity in its outflow phase, and it now excites a small reflection nebula. One study found this star is of intermediate mass ($> 3M_{\odot}$), with a luminosity of 84 $L_{\odot}$ (Hessman et al. 1995). Optical and near-infrared photometry are consistent with pure photospheric emission from this star. The new Spitzer data extend this photospheric emission out to 8 μm and do not detect the star at all at 24 μm: we conclude the star has no circumstellar disk.

A second pre-main-sequence star resides within the cavity with LkHα 349a; we will refer to it as LkHα 349c, and it was first noted by Cohen & Kuhi (1979). While LkHα 349c is 1.5 mag fainter than LkHα 349a in the visible, it is much brighter in the infrared. A small excess over photosphere is evident at 3.6 μm; it is very significant (1.9 mag) at 8 μm; and by 24 μm there is negligible emission from the photosphere. Thus these two pre-main-sequence stars are in very different stages of evolution, with LkHα 349a having cleared its disk and LkHα 349c still harboring a massive disk. Comparing optical photometry to Siess et al. (2000) tracks yields an age of 2.0 Myr for LkHα 349c. The star Tr 37 11-2146, labeled in Figure 2, is also detected with a strong infrared excess suggesgting its youth. Ultraviolet observations also reveal a strong excess, and the inferred accretion rate $\sim 10^{-7} M_{\odot}$ yr^{-1} (Sicilia-Aguilar et al. 2004). Most low-mass Tr 37 cluster members are 3–5 Myr old (Sicilia-Aguilar et al. 2004); if infrared excess is indicative of youth, then we expect the infrared-selected sample to be younger.

Three B stars are located in or near the globule: HD 205948 (B2V) is just north of the globule head, and HD 205794 (B0.5V) is west of the globule head, and HD 239710 (B3V) is projected in front of the globule, just east of IC 1396:θ. All of these stars are surrounded by 24 μm nebulosity, with in-band luminsoity $\sim 0.04 L_{\odot}$, though the stars themselves are not detected at 24 μm. We interpret these nebulae as molecular cloud dust heated by the stars. From Spitzer, L. (1978), the the dust is expected to be heated mostly by direct stellar radiation (and only a small contribution from scattered Lyα), with Strömgren sphere radii $\sim$ 0.01–0.1$(10^3/n)^{2/3}$ pc, comparable to the observed nebula sizes. That the Spitzer, L. (1978) models roughly correspond to the observations suggests *Spitzer* is a very sensitive instrument for identifying B-star H II regions/reflection nebulae.

5. Protostars

One of the most remarkable aspects of the *Spitzer* images is the presence of numerous, bright mid-infrared sources with faint or no counterpart at shorter wavelengths. To find near-infrared counterparts, we used post-survey data from the 2MASS project, which observed the Elephant Trunk Nebula to a depth 6-times the nominal survey. The brightest optical and 2MASS stars are seen in all the IRAC images, and even relatively faint stars at 3.6 μm. But the correspondence between optical and near-infrared sources and 8 μm sources is poorer, and by 24 μm the field is unrecognizable. There are four *IRAS* sources in the region, all 'detected' at 25 μm. One of these corresponds to the brightest *Spitzer* source α, but with 25 μm flux twice as high (due to globule contamination). Another is the infrared-bright T Tauri star that is the southernmost bright source in the *Spitzer* image. The other two *IRAS* sources are spurious; the *Spitzer* image shows bright but diffuse 24 μm emission.

Figure 3 shows the *Spitzer* color-color diagram for the 24 μm-detected sources. Few of the sources are dominated by stellar photospheres, which would concentrate near [8]-[24]=[3.6-5.8]=0 since the foreground extinction is small. The sources to the upper-right are the reddest and likely youngest protostars. There is a sequence of these protostars progressing roughly toward the main sequence but noticeably offset such that upon arriving at photospheric [3.6]-[5.8] color, the young stars still retain significant disks. A separate set of sources has photospheric [3.6]-[5.8]$\sim$ 0 but significant 24 μm excess; these are 'debris disk' candidates. Some of these may actually be young stars with massive disks with inner holes—thus lacking the warmer dust that produces the shorter-wavelength emission. Others are main sequence stars with debris disks due to collisional comminution of their asteroids and comets. For reference, the debris disk around β Pic has [3.6]-[5.8]=0.0, [8]-[24]=3.3. Some of the sources with extremely large 24 μm excesses, are actually contamination by globule material; inspecting some of the points in the lower-right portion of the indicates their 24 μm emission is likely globule contamination.

Fourteen potential protostars were studied in detail; they are labeled with Greek letters in Figure 2 and listed in Table 1. The sources were selected first by inspecting the 24 μm image, then by verifying that none of the automatically-detected sources were missed. IRAC magnitudes were calculated using a 5.4″ radius aperture with respect to a reference annulus from 6 to 9″. An aperture correction of 1.07, 1.08, 1.08, and 1.10 was applied to 3.6, 4.5, 5.8, and 8 μm, respectively, to raise values to the standard calibration aperture of 12″. MIPS magnitudes are within an aperture of 12″ with an aperture correction of 1.15. Mid-infrared luminosities, L_{MIR} ($L_\odot$), were calculated by integrating the spectral energy distribution from 3.6 to 24 μm (with linear interpolation between the observed wavelengths). We measured the full width at half-maximum (FWHM) intensity of each source at 24 and 3.6 μm, to verify

they are point-like at the intstrumental resulution. All sources in Table 1 are unresolved at 24 μm, with 5.2″ median FWHM equal to that of the PSF. The IRAC 3.6 μm point spread function has a FWHM of 1.6″ in a drizzled reconstruction at 0.3″ pixel scale. All but two sources are between 1.5 and 2.1″, consistent with being true point sources. The remaining two sources, α and ξ, are 2.4″ in apparent size, but they are both blended with nearby stars and are probably not truly resolved.

Figure 4 shows the spectral energy distributions of 5 new protostars and the two T Tauri stars. The sources form a relatively clear sequence with the mid-infrared emission decreasing as the near-infrared emission increases, obviously suggestive of an evolutionary sequence wherein the stars are gradually dispersing their envelopes. Comparing to the colors of pre-main sequence objects in the Taurus-Auriga molecular cloud, we classified the objects as per the criteria in Kenyon & Hartmann (1995) and Wilking et al. (1989). Eight of the sources in Table 1 are Class 0, I or flat-spectrum protostars. Eight of the sources in Table 1 (including LkHα 349c and another star), and 47 overall, have mid-infrared colors of Class II objects. The spectral energy distribution of source β in Figure 4 clearly shows a faint, barely-emerging photosphere. The 8 μm data points may be slightly depressed due to a silicate absorption feature, which can be very deep for protostars (Gibb et al. 2003); spectroscopy is needed to understand these objects in more detail. Nearly all of the *Spitzer*-detected objects are in very early stages, where the direct luminosity from the photosphere is dwarfed by that of its envelope or disk.

6. Discussion and Conclusions

The new *Spitzer* images of the Elephant Trunk Nebula significantly alter our understanding of its nature from a dark, cold globule containing only two T Tauri stars into a cauldron of protostars. The mass of molecular gas in the globule was estimated from independent observations to be $220 M_\odot$ from a high-resolution CO map (Patel et al. 1995), $170 M_\odot$ from the ^{12}CO and $90 M_\odot$ from ^{13}CO (Weikard et al. 1996), and $< 30 M_\odot$ from a coarse ^{13}CO map (Dobashi et al. 1996); we will adopt $\sim 200 M_\odot$. The globule mass is much less than the Virial mass, estimated at 300–800 $M_\odot$ (Patel et al. 1995; Weikard et al. 1996), suggesting it would be quiescent and transient and *not* subject to gravitational collapse if it were in isolation—instead, it would dissipate in a crossing time $\sim 5 \times 10^5$ yr. Including the pressure of the surrounding material only slightly increases the lifetime.

While we do not know the masses of the individual protostars, we can get an order-of-magnitude estimate of their total mass by assuming the average protostar is 0.5 $M_\odot$, yielding a current protostellar mass of $\sim$ 8–30 $M_\odot$, where the lower estimate includes only

Class I sources and the upper limit includes Class II. The fraction of the globule currently in detected protostars is 4–15 %, similar to other emdebbed clusters (Lada & Lada 2003). Assuming an age $\sim 10^5$–10^6 yr for the Class I–II protostars (André, Ward-Thompson, & Barsony 2000), the star formation rate $\dot{M}_* \sim 10^{-4} M_\odot$ yr^{-1}, with the relative populations of Class I and II consistent with their ages and spatial distributions. (The Class I sources are mostly located in the dense globule and in particular along its rim, while the Class II sources are more widely distributed.) The globule could supply material to form stars at this rate for only $M/\dot{M}_* \sim 2 \times 10^6$ yr, comparable to the lifetime for photoevaporation of the globule by the O6 star, $\sim 2 \times 10^6$ yr (Lefloch & Lazareff 1994). Coincidentally, the globule lifetimes, comparable to the main-sequence lifetime of the O6 star.

The location of protostars—within a globule that is clearly being illuminated and shaped by a nearby O star—and the high specific star formation rate and concentration of so many young objects in a small volume all suggest that the Elephant Trunk Nebula protostars were triggered to form in a cloud that may not have formed many stars had it not been acted upon by external forces. The new protostars IC 1396A:γ and IC 1396A:δ and IC 1396A:ϵ in particular have extremely red mid-infrared spectral energy distributions indicating their youth. The generation of stars we are presently witnessing is likely to be the last produced by this globule, because it will likely be photoevaporated by the nearby O6 star before more stars can form.

This work is based in part on observations made with the *Spitzer Space Telescope*, which is operated by the Jet Propulsion Laboratory, California Institute of Technology under NASA contract 1407. Support for this work was provided by NASA through an award issued by JPL/Caltech. This publication makes use of data products from the Two Micron All Sky Survey, which is a joint project of the University of Massachusetts and the Infrared Processing and Analysis Center/California Institute of Technology, funded by the National Aeronautics and Space Administration and the National Science Foundation.

REFERENCES

André, P., Ward-Thompson, D., & Barsony, M. 2000, in *Protostars and Planets IV*, eds. V. Mannings, A. P. Boss, & S. S. Russell (Tucson: University of Arizona Press), 59

Boulanger, F., Lorente, R., Miville-Deschênes, M. A., Abergel, A., Blommaert, J., Cesarsky, D., Okumura, K., Pérault, M., & Reach, W. T. 2004, Mid-IR Spectro-imaging ISOCAM CVF Observations, Infrared Space Observatory Data Archive [paper in preparation]

Cohen, M., & Kuhi, L. V. 1979, ApJS, 41, 743

Dobashi, K., Bernard, J.-P., & Fukui, Y. 1996, ApJ, 466, 282

Froebrich, D., & Scholz, A. 2003, A&A, 407, 207

Gibb, E. L., Whittet, D. C. B., Schutte, W. A., Boogert, A. C. A., Chiar, J. E., Ehrenfreund, P., Gerakines, P. A., Keane, J. V., Tielens, A. G. G. M., van Dishoeck, E. F., & Kerkhof, O. 2003, ApJ, 536, 347

Fazio, G. G. et al. 2004, ApJS, THIS VOLUME

Herbig, G. H., & Bell, K. R. 1988, *Lick Obs. Bull.*, 1111

Hessman, F. V., Beckwith, S. V. W., Bender, R., Eislöffel, J., Götz, W., & Guenther, E. 1995, A&A, 299, 464

Ingalls, J. G., et al. 2004, ApJS (this volume)

Kenyon, S. J., & Hartmann, L. 1995, ApJS, 101, 117

Lada, C. J., & Lada, E. A. 2003, ARA&A, 41, 57

Lefloch, B., & Lazareff, B. 1994, A&A, 289, 559

Morbidelli, L., Patriarchi, P., Perinotto, M., Barbaro, G., & Di Bartolomeo, A. 1997, A&A, 327, 125

Moriarty-Schieven, G. H., Xie, T., & Patel, N. A, ApJL, 463, L105

Nakano, M., Tomita, Y., Ohtani, H., Ogura, K., & Sofue, Y. 1989, PASJ, 41, 1073

Osterbrock, D. E. 1974, *Astrophysics of Gaseous Nebulae* (San Francisco: Freeman).

Patel, N. A., Goldsmith, P. F., Snell, R. L., Hezel, T., & Xie, T. 1995, ApJ, 447, 721

Reipurth, B., Armond, T., Raga, A., & Bally, J. 2003, ApJL, 593, L47

Rho, J., Jarrett, T. H., Cutri, R. M., & Reach, W. T. 2001, ApJ, 547, 885

Rieke, G. H. et al. 2004, ApJS, THIS VOLUME

Sicilia-Aguilar, A., Hartmann, L. W., Briceño, C., Muzerolle, J., & Calvet, N. 2004, submitted

Siess, L., Dufour, E., & Forestini, M. 2000, A&A, 358, 593

Spitzer, L. *Physical Processes in the Interstellar Medium* (New York: Wiley)

Weikard, H, Wouterloot, J. G. A., Castets, A., Winnewisser, G., & Sugitani, K. 1996, A&A, 309, 581

Werner, M. W. et al. 2004, ApJS, THIS VOLUME

Wilking, B. A., Lada, C. J., & Young, E. T. 1989, ApJ, 340, 823,

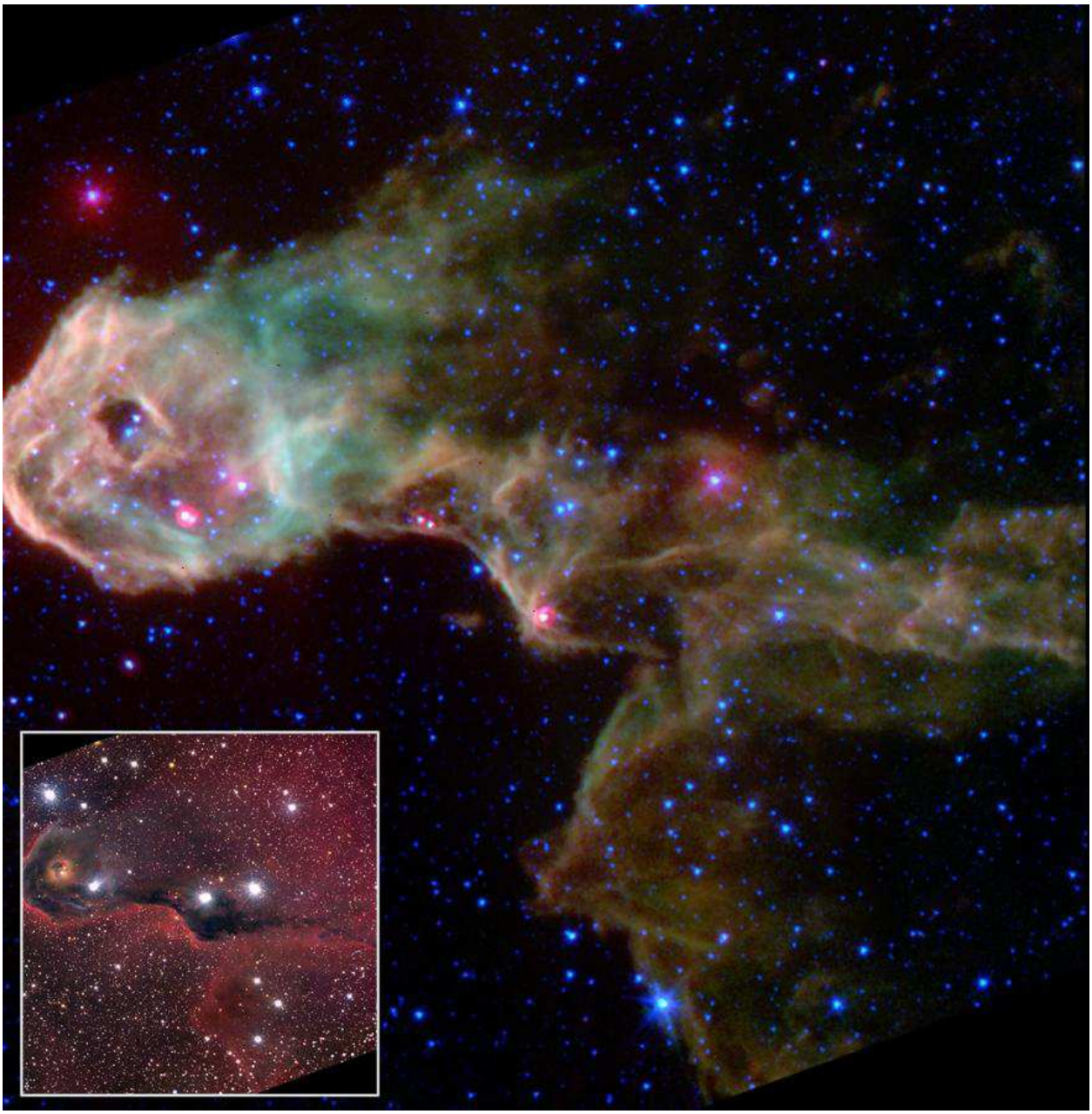

Fig. 1.— [COLOR PLATE] *Spitzer* image of the Elephant Trunk Nebula in IC 1396, combining the MIPS 24 μm (red) and IRAC 5.8+8 μm (green) and 3.6+4.5 (blue) μm images. The inset shows the optical image, combining red, green, and blue images from the CFHT. This figure is available as an animation in the electronic edition of the *Astrophysical Journal*. The animation begins with the CFHT image and transforms into the *Spitzer* image with each time-step moving to progressively longer wavelength. North is rotated 13° from vertical. The total horizontal image size is 17.6′.

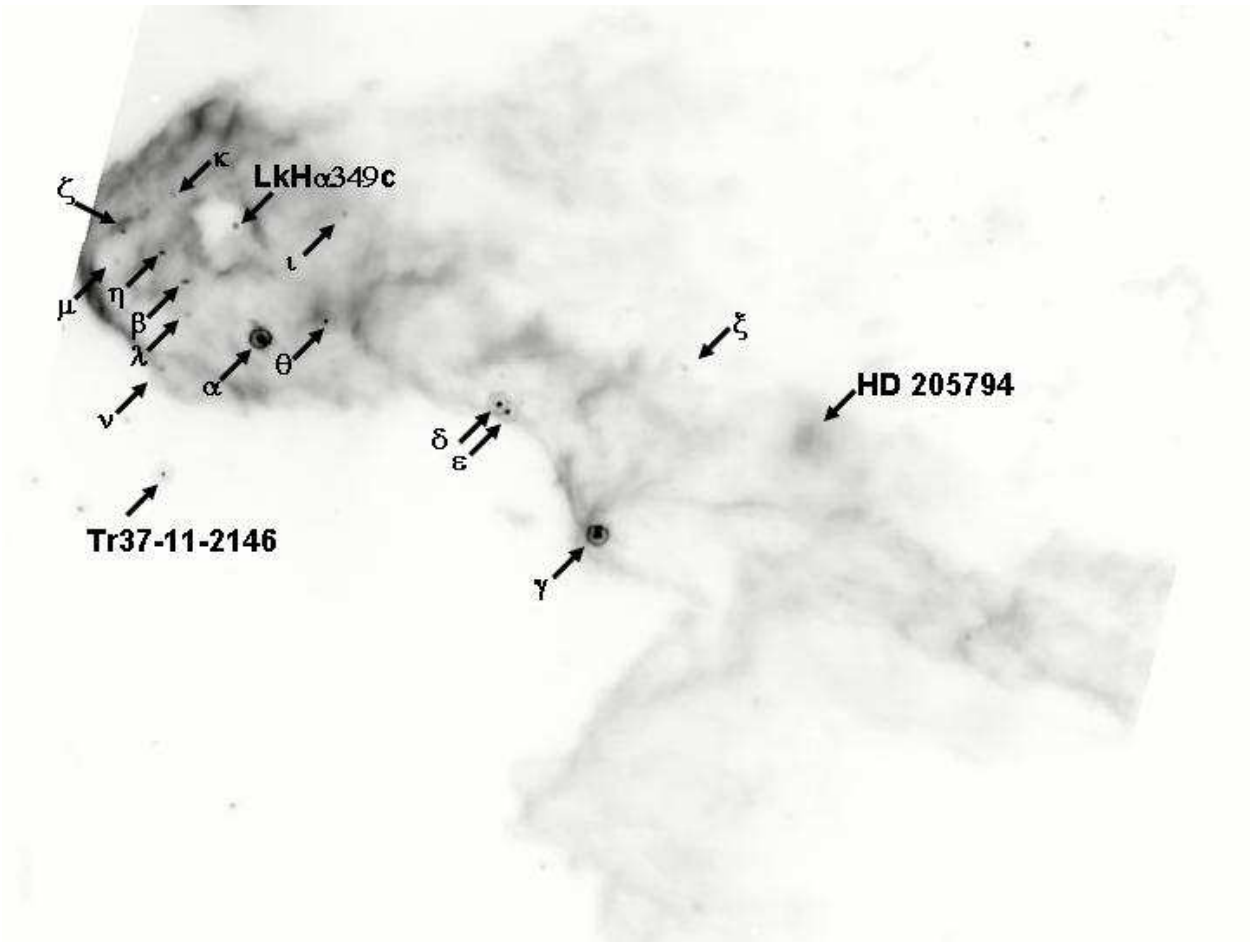

Fig. 2.— *Spitzer*/MIPS 24 μm image of the Elephant Trunk Nebula with newly discovered sources (α–ξ) labeled. North is up and east is left.

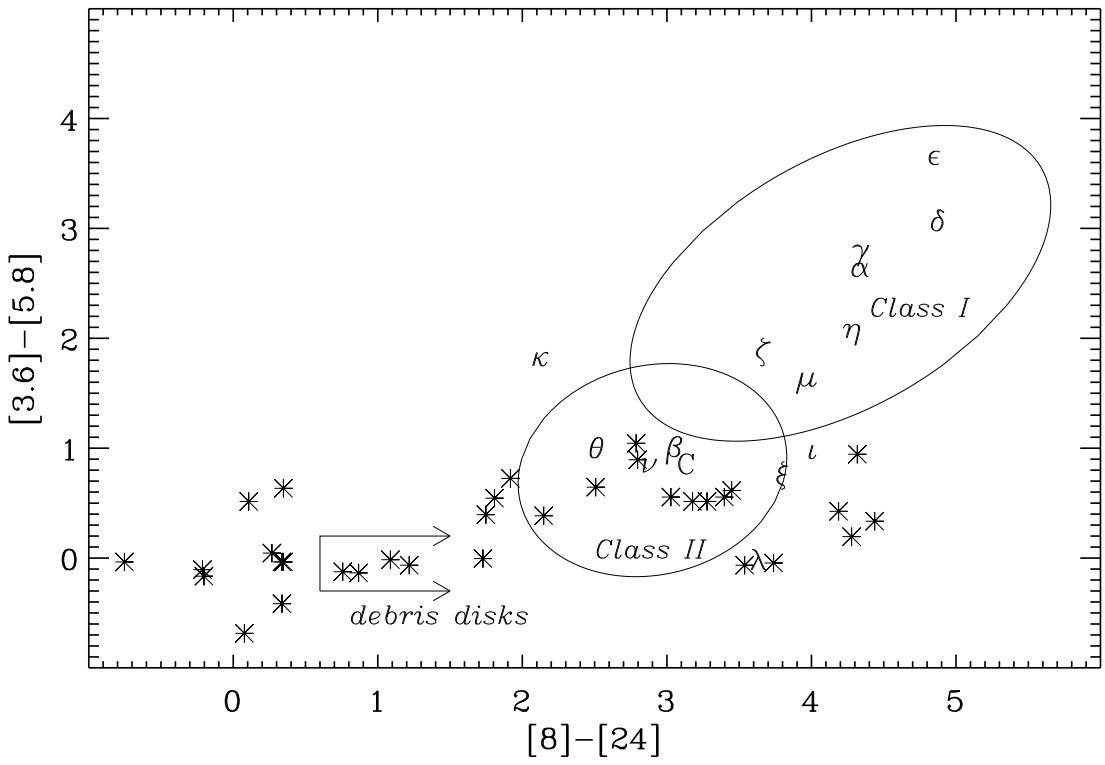

Fig. 3.— *Spitzer* color-color diagram for 24 μm-detected sources in the Elephant Trunk Nebula (IC 1396A). Labeled points are from Table 1. The approximate locations of Classes I and II protostars and main sequence stars with debris disks are outlined.

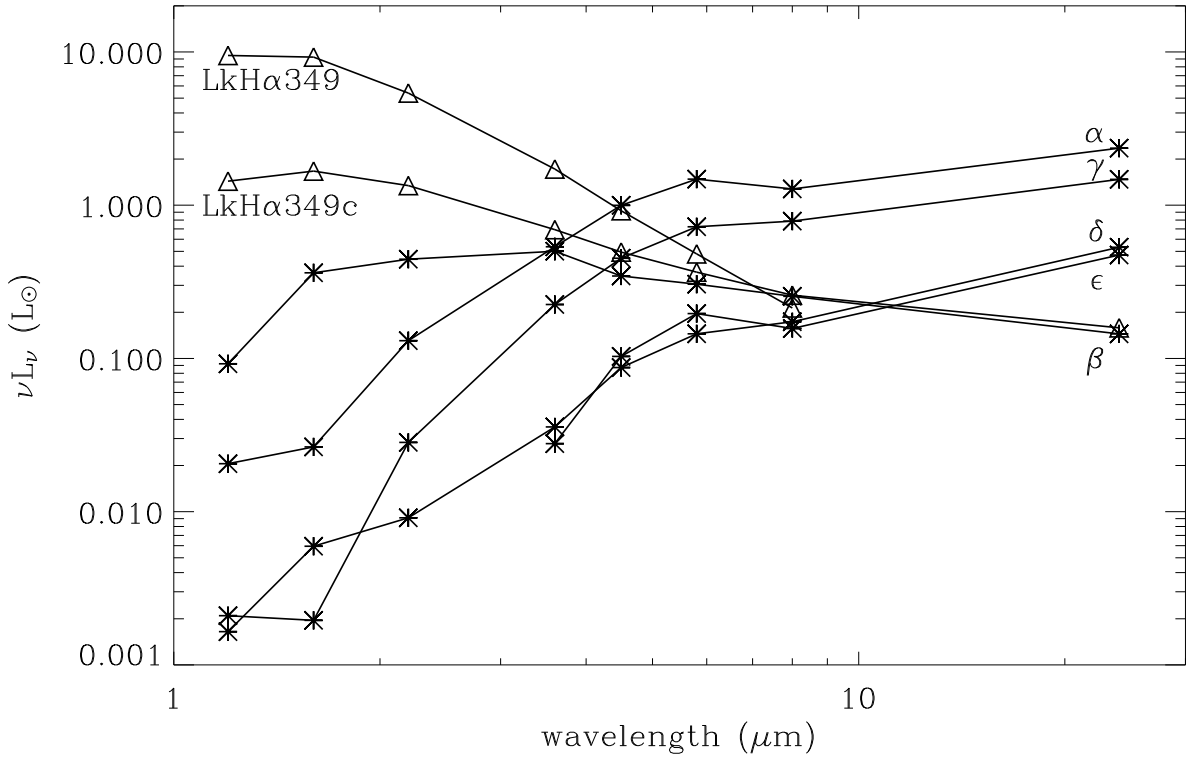

Fig. 4.— Spectral energy distributions for 5 newly-discovered protostars (α–ϵ) and the two previously-known young stars (LkHα 349 a and c). The spectrum of LkHα 349a provides a reference for photospheric emission, while the others show varying degrees of infrared excess.

Table 1. Photometry of young stellar objects in the Elephant Trunk Nebula

name	Class	RA [21^h]	Dec [57°]	[24]	[8]	[5.8]	[4.5]	[3.6]	K_s	H	J	L_{MIR}
α	I	$36^m46.5^s$	$29'38''$	2.01	6.28	7.13	8.30	9.70	12.66	15.31	16.37	2.8
β	II	$36^m55.1^s$	30 29	5.04	8.03	8.85	9.46	9.77	11.33	12.47	14.74	0.5
γ	I/0	$36^m07.8^s$	26 36	2.52	6.80	7.91	9.17	10.64	14.32	...	...	1.6
δ	I/0	$36^m19.2^s$	28 38	3.63	8.44	9.66	10.95	12.64	15.55	...	...	0.5
ϵ	I/0	$36^m18.2^s$	28 31	3.75	8.55	9.33	10.77	12.91	...	...	...	0.4
ζ	I	$37^m02.2^s$	31 15	4.46	8.06	9.02	9.86	10.84	13.62	16.48	...	0.5
η	I	$36^m57.7^s$	30 55	4.93	9.15	10.25	11.33	12.25	...	...	...	0.2
θ	II	$36^m39.0^s$	29 52	4.07	6.53	7.25	7.67	8.16	9.50	10.21	12.02	2.0
ι	II	$36^m36.8^s$	31 32	5.63	9.60	10.19	10.74	11.10	12.01	12.58	13.82	0.2
κ	II	$36^m56.4^s$	30 00	8.10	10.17	10.76	11.71	12.51	13.46	15.00	17.67	0.1
λ	If	$36^m54.8^s$	30 00	5.91	9.48	10.20	9.92	10.09	13.77	15.72	...	0.2
μ	I	$37^m02.9^s$	31 51	7.47	11.36	12.60	12.29	14.17	...	...	...	0.1
ν	I/II	$36^m57.8^s$	29 10	5.77	8.58	9.43	9.92	10.21	15.83	14.17	13.41	0.3
ξ	I/II	$35^m57.8^s$	29 11	6.67	10.42	12.38	12.58	13.07	14.81	...	...	0.1
Tr 37 11-2146	II	$36^m57.5^s$	27 33	5.21	8.34	9.12	9.41	9.87	10.82	11.52	12.54	0.4
Lk Hα 349a	III	$36^m49.3^s$	31 21	...	8.22	8.35	8.39	8.43	8.62	8.95	9.71	0.7
Lk Hα 349a	II	$36^m50.6^s$	31 10	4.94	8.01	8.65	9.07	9.42	10.13	10.81	11.76	0.6